Effect of Post-Deposition Annealing Temperature on H2S Sensing and Low-Frequency Noise Characteristics of In_2O_3 Gas Sensor

Wonjun Shin, Seongbin Hong, Yujeong Jeong, Gyeweon Jung, Jinwoo Park, Donghee Kim, Byung-Gook Park, Jong-Ho Lee,

Department of Electrical and Computer Engineering and Inter-University Semiconductor Research Center, Seoul National University, Seoul, 151-742, Republic of Korea
Phone: +82-2-880-1727 E-mail: jhl@snu.ac.kr

Abstract

In this work, effects of post-deposition annealing (PDA) temperature on H2S gas sensing and low-frequency noise (LFN) characteristics of In_2O_3 gas sensor are investigated. Considering both response and LFN of the sensor, signal-to-noise-ratios (SNRs) of the sensors post-annealed at different temperatures are demonstrated and the optimal PDA temperature is suggested. The results show that the noise plays a dominant role in determining the SNR of sensors.

1. Introduction

Metal-oxide (MOX) based gas sensors are considered as the most attractive candidates for gas sensor applications, owing to their sufficient response and simple fabrication process [1]. For a long time, there have been significant efforts to improve the performance of the MOX gas sensors and most of them are focusing on improving the response of the sensors [1]. However, only limited knowledge is available about the low-frequency noise (LFN) characteristics of the sensors, which determines the signal-to-noise-ratio (SNR), limit of detection, and signal resolution of the sensors [2]. Post-deposition annealing (PDA) temperature of the sensor is one of the important factors that affect the gas sensing properties of sensors [3]. However, there have been no researches about the effects of PDA condition on LFN characteristics and SNR of sensors. In this work, we investigate the H2S gas sensing properties, LFN characteristics, and SNR of In_2O_3 gas sensors at different PDA temperatures.

2. Sensor fabrication

On the top of the metal electrodes (TiN/Al/TiN/Ti (10 nm/50 nm/10 nm/10 nm)), In_2O_3 thin films are deposited. In_2O_3 films are prepared by radio frequency (RF) magnetron sputtering method using an In_2O_3 target (99.99%(4N)). The target is pre-sputtered for 40 mins before the deposition. During the deposition, the argon/oxygen flow rate, substrate temperature, and sputtering pressure are set to 30 sccm/3 sccm, 20 °C, and 5 mTorr, respectively. After the deposition, In_2O_3 films are subjected to thermal annealing at 200 °C, 300 °C, and 400 °C in vacuum. Fig. 1 (a) and the insert show the top SEM the sensor and In_2O_3 thin film post-annealed at 200 °C. Fig. 1 (b) shows the sheet resistance (R_{SHEET}) of the In_2O_3 film as a function of PDA temperatures. When the PDA temperature increases, the amount of oxygen vacancy increases, which increases the carrier concentration [4]. Also, a grain boundary scattering decreases with increasing grain size [4]. Therefore, the R_{SHEET} decreases with increasing PDA temperature.

3. Gas sensing and LFN characteristics

Fig. 2 (a) shows transient response behaviors of the sensors at a fixed H2S gas concentration of 125 ppm as a function of PDA temperature. H2S gas is injected into the test chamber at 30 s and dry air is injected at 130 s for the recovery. The gas response is measured at 220 °C. In_2O_3 film post-annealed at 200 °C has the largest surface-to-volume-ratio due to the smallest grain size and thus the largest response. Fig. 2 (b) shows the responses of In_2O_3 sensors annealed at different temperatures to 125 ppm of H2S gas as a function of operating temperatures. The sensors show the same optimal operating temperature of 220 °C.

Fig. 3 shows the normalized current noise spectral densities (S_I/I^2s) of the sensors post-annealed at different temperatures. The S_I/I^2s are measured in a dry air ambience at 220 °C. The sensors show $1/f^{\gamma}$ noise behavior where γ is denoted as $-\partial \ln S / \partial f$. It has been reported that carrier mobility fluctuation due to a carrier scattering at the grain boundary is the origin of the $1/f$ noise in polycrystalline resistor [5]. In order to verify whether there is a noise source other than the CMF at the grain boundary, the tendency of S_I/I^2 to R_{SHEET} is investigated. The proportionality of the S_I/I^2 to R_{SHEET} or R_{SHEET}^2 is interpreted as an indication of whether the LFN originates from the bulk or the interface [6]. Fig. 4 shows the log-log plot of R_{SHEET} versus S_I/I^2 of the sensors post-annealed at different temperatures. The result demonstrates that the origin of the $1/f$ noise shifts from the interface to the bulk of In_2O_3 with increasing annealing temperature. It seems that excess RF sputtering power damages the interface and increases the carrier number fluctuation at the interface. During the PDA, the damaged interface is recovered, but the annealing temperature of 200 °C does not fully recover the damaged interface. In the fields of gas sensor studies, the importance of the surface and bulk properties of the MOX based sensing material has been widely recognized. However, the results demonstrate that the interface quality also affects the noise of the sensor, and thus the sensing performance such as LFN characteristics. Fig. 5 (a) shows SNR as a function of PDA temperature. Although the sensor post-annealed at 200 °C shows the largest response, it shows the smallest SNR due to interface-related noise. SNR is constant regardless of

operating voltage, as shown in the Fig. 5 (b). Fig. 6 shows the SNR of the sensors post-annealed at different temperatures as a function of H2S gas concentration. The equation at the bottom shows the power-law dependence between the H2S gas concentration and SNR.

4. Conclusions

We have investigated the H2S gas sensing and low-frequency noise characteristics of In2O3 sensors post-annealed at different temperatures. The sensor post-annealed at the 200 ℃ shows the largest response due to the smallest grain size, which has the largest surface-to-volume-ratio. However, the sensor also has the largest noise due to the noise related to the damaged interface between the sensing material and the substrate. Therefore, the sensor post-annealed at 200 ℃ shows the worst SNR performance. The results demonstrate that not only the response but also the low-frequency noise characteristics should be considered in designing sensors with optimal performance.

References
[1] N. Barsan, et al, Sens. Actuators B Chem. **121** (2007) 18.
[2] N. K. Rajan, et al, Appl. Phys. Lett. **98** (2014) 264107.
[3] Y. Hu et al, Sens. Actuators B Chem. **108** (2005) 244.
[4] Z. Yuan et al, Thin Solid Films **519**, (2011) 3254.
[5] K. M. Chen et al, Appl. Phys. Lett. **81** (2002) 2578.
[6] P. Dutta et al, Rev. Mod. Phys. **53** (1981) 497.

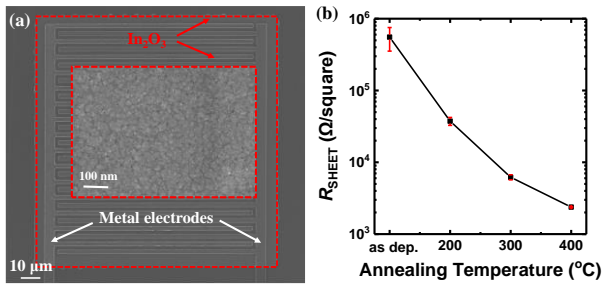Fig. 3. Normalized current noise spectral densities (S_I/I^2s) of the sensors annealed at different temperatures. The S_I/I^2s are measured in a dry air ambience at 220 ℃. The γ values of the sensors annealed at 200 ℃, 300 ℃, and 400 ℃ are 1.34, 1.33, and 1.36, respectively.

Fig. 4. Log-log plot of R_{SHEET} versus S_I/I^2 of the sensors annealed at different temperatures. The origin of the $1/f$ noise shifts from the interface to the bulk of In2O3 with increasing annealing temperature.

Fig. 5. (a) SNR as a function of annealing temperature. SNR of the sensor is the largest when PDA temperature is 300 ℃. (b) SNR as a function of voltage (V) applied to the electrodes of the sensor. SNR is constant regardless of operating voltage

Fig. 1. (a) Top SEM image of the sensor post annealed at 200 ℃. The size of sensing area is 100×125 μm. The insert shows the SEM image of In2O3 thin film. (b) Sheet resistance (R_{SHEET}) of the sensors as a function of PDA temperature.
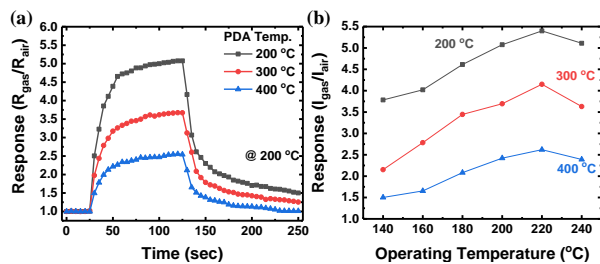

Fig. 2. (a) Transient response behaviors of the sensors as a function of PDA temperature. H2S gas is injected into the test chamber at 30 s and dry air is injected at 130 s for the recovery. (b) Responses of the sensors postannealed at different temperatures to 125 ppm of H2S gas as a function of operating temperatures.
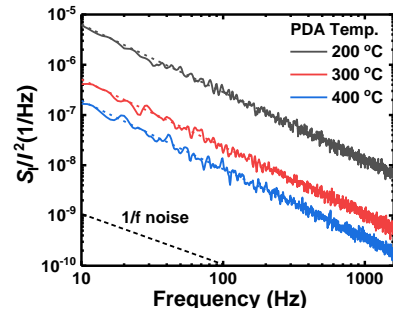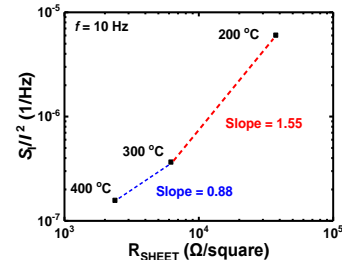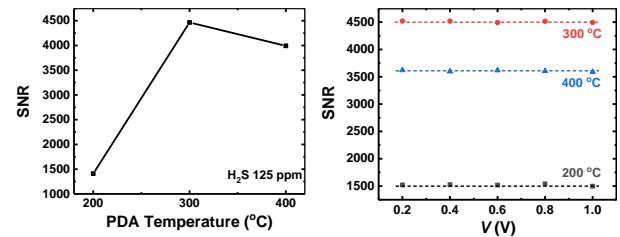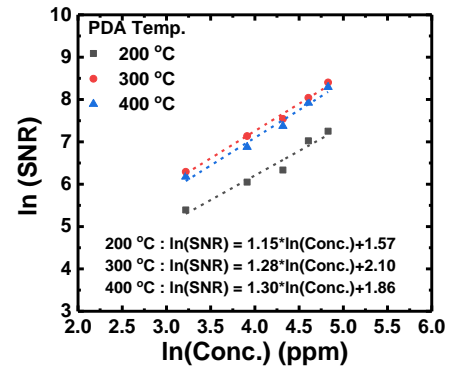

Fig. 6. SNR of the sensors post-annealed at different temperatures as a function of H2S gas concentration. The equations at the bottom show the power-law dependence between the H2S gas concentration and SNR.